RESEARCH   **Open Access**

Quantum wire with parallelogram cross section: optical properties

Reza Khordad[1]

Abstract

In the present work, the optical properties of a GaAs quantum wire with a parallelogram cross section are studied. In this regard, we have used the expressions for the optical properties obtained by the compact-density matrix formalism. Here, we have investigated the intersubband optical absorption coefficients and refractive index changes as a function of the structure parameter of the wire (side length) and the incident optical intensity. According to the obtained results, it is found that (1) the total refractive index changes increase and shift towards lower energies when the side length increases and that (2) the total absorption coefficient decreases as the side length increases. Also, the resonance peak shifts towards lower energies by increasing the side length.

Keywords: Quantum wire, Optical properties, Absorption coefficient

PAC Codes: 78.67.-n; 78.67.Lt

Background

The studies on the physics of low-dimensional semiconductor structures open a new field in fundamental science such as chemistry, physics, and engineering. Examples of these structures are superlattices, quantum wires, single and multiple quantum wells, and quantum dots [1-7]. The physical properties of these structures have been extensively studied both experimentally and theoretically [1,2]. The structures confine charge carriers in one, two, and three dimensions. Quantum confinement of the charge carriers in these structures leads to the formation of discrete energy levels, the enhancement of the density of states at specific energies, and the drastic change of optical absorption spectra.

One of the most intensively explored classes of semiconductor structures is the class of quantum wires. With technological progresses in the fabrication of semiconductor structures like chemical lithography, molecular beam epitaxy, and etching, it has been made possible to fabricate a wide variety of quantum wires with well-controlled

shape and composition. Among heterostructures, quantum wires with rectangular, T-shaped, V-groove, triangular, and other cross sections have received lots of attention by researchers during the last decade [4-7].

The linear and nonlinear optical properties of low-dimensional semiconductor structures are of considerable current interest in connection with their potential applications in optoelectronic and photonic devices [8, 9]. It is worth mentioning that there are many novel optical properties in the low-dimensional semiconductor structures which are not in their bulk materials [10-12]. The linear and nonlinear optical properties of nanostructures have been widely studied theoretically by several authors [13, 14].

The linear intersubband optical absorption within the conduction band of a GaAs quantum well without and with an electric field has been experimentally studied [15, 16]. Nonlinear intersubband optical absorption in a semiconductor quantum well also was calculated by Ahn and Chuangin [17]. In 1991, Rappen et al. [18] studied the nonlinear absorption for two-dimensional magnetoexcitons in $In_xGa_{1-x}As/In_yAl_{1-y}As$ quantum wells. In 1992, Bockelman and Bastard [19] discussed interband absorption in quantum wires with a magnetic field case and without a magnetic field case [20]. Intersubband optical absorption in coupled quantum wells under an applied electric field was studied by Yuh and Wang [21]. In 1993, Cui et

Correspondence: khordad@mail.yu.ac.ir
[1] Department of Physics, College of Sciences, Yasouj University, Yasouj, 75914-353, Iran

al. [22] experimentally studied the absorption saturation of intersubband optical transitions in GaAs/AlxGa$_{1-x}$As multiple quantum wells. Recently, we have studied the optical properties of a quantum disk in the presence of an applied magnetic field [23]. Also, we have investigated the optical properties of a modified Gaussian quantum dot under hydrostatic pressure [24].

In the last years, the intersubband optical absorption coefficients and refractive index changes in nanostructures have attracted considerable and continuous attention [25]. For example, Wang et al. [26] examined the refractive index changes induced by the incident optical intensity in a semiparabolic quantum well. Ünlü et al. [27] investigated the optical rectification in a semiparabolic quantum well. To obtain information about the optical properties of low-dimensional systems, the reader can refer to [28-31].

In this paper, we intend to study the optical absorption coefficients and refractive index changes of a quantum wire with a parallelogram cross section. The theory and calculations are briefly presented in the 'Theory and model' section. Analytical expressions for the linear and nonlinear intersubband optical absorption coefficients and refractive index changes are presented in the 'Optical absorption coefficients and refractive index changes' section. The results and discussion are presented in the 'Results and discussion' section.

Results and discussion

In this section, we have carried out the numerical calculations for a GaAs parallelogram quantum wire. The used parameters in the present work are as follows: $n_r = 3.2$, $T_{12} = 0.2$ ps, $\Gamma_{12} = 1/T_{12}$, and $\sigma_v = 3.0 \times 10^{16}$ cm^{-3}.

In Figure 1, we have presented the typical cross section of a parallelogram quantum wire.
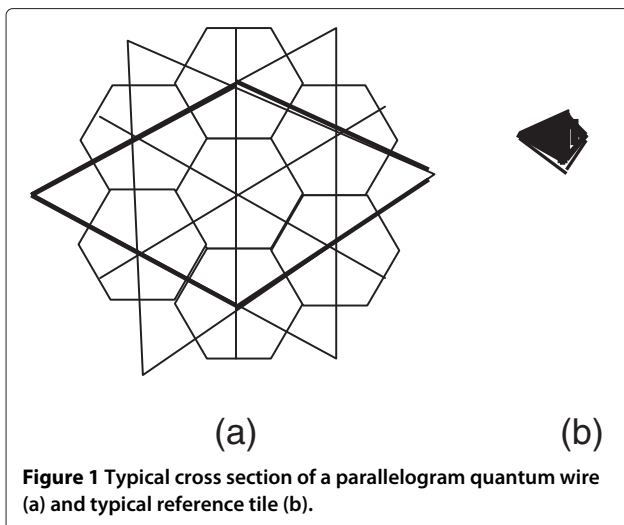

Figure 1 Typical cross section of a parallelogram quantum wire (a) and typical reference tile (b).
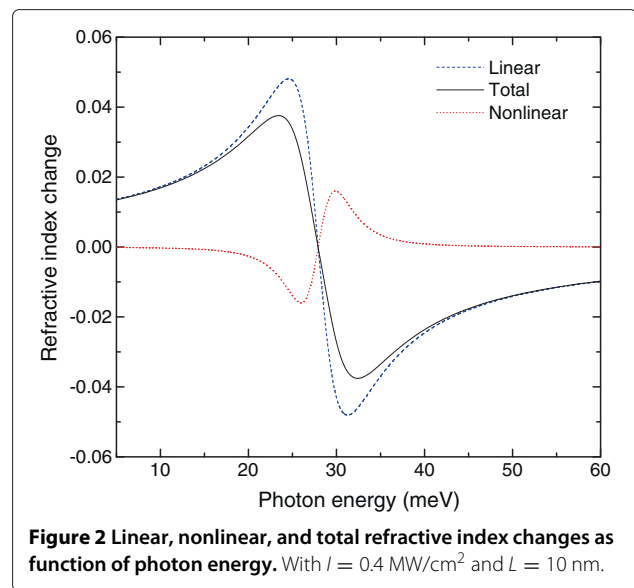

Figure 2 Linear, nonlinear, and total refractive index changes as function of photon energy. With $I = 0.4$ MW/cm^2 and $L = 10$ nm.

Figure 2 shows the linear, nonlinear, and total refractive index changes as a function of the photon energy with $I = 0.4$ MW/cm^2 and $L = 10$ nm. The linear and nonlinear terms are of opposite signs. Therefore, the total refractive index change decreases. It is clear that the nonlinear term is strongly dependent on the incident optical intensity. Therefore, the cancelation of the nonlinear term for the system operating with a high incident optical intensity cannot be correct.

In Figure 3, we have plotted the total refractive index change as a function of the photon energy for four different incident optical intensities as 0, 0.1, 0.2, and 0.3 MW/cm^2 with $L = 10nm$. It is seen from the figure that
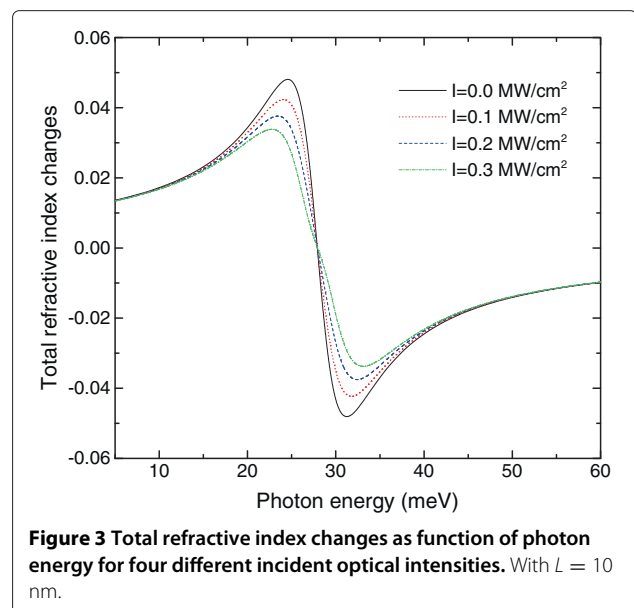

Figure 3 Total refractive index changes as function of photon energy for four different incident optical intensities. With $L = 10$ nm.

the total refractive index change reduces when the incident optical intensity increases. As we know, the linear term does not depend on the incident optical intensity, but the nonlinear term changes with optical intensity. Therefore, the higher optical intensity will cause to increase the nonlinear term and increase the difference between them. Since these two terms are of opposite signs, the total change reduces.

Figure 4 displays the total refractive index changes as a function of the photon energy for three different lengths as $L = 10, 11$, and 12 nm with $I = 0.4$ MW/cm^2. It is observed from the figure that the total refractive index changes will be decreased as the quantum size L decreases. It is clear that the refractive index change is dependent on the dipole matrix elements M_{ij}. By decreasing L, the wave function associated with the electron is more compressed and localized. Therefore, the dipole matrix elements and, thereby, the refractive index changes reduce. From the figure, it is seen that the resonance peak position shifts towards higher energies with decreasing quantum size L. The main reason for this behavior is the increase of the quantum confinement with decreasing L. Also, the energy difference between two electronic states increases by decreasing L. Therefore, the resonance peak position shifts towards higher energies.

Figure 5 displays the linear, nonlinear, and total absorption coefficients as a function of the photon energy with $I = 0.4$ MW/cm^2 and $L = 10$ nm. It is seen from the figure that there is a resonance peak at a photon energy which relates to the energy difference between the levels considered. The linear and nonlinear absorption coefficients are of opposite signs. Therefore, the total absorption coefficient decreases. It is obvious that the nonlinear absorption coefficient is dependent on the incident optical intensity,

Figure 5 Linear, nonlinear, and total absorption coefficients as function of the photon energy. With $I = 0.4$ MW/cm^2 and $L = 10$ nm.
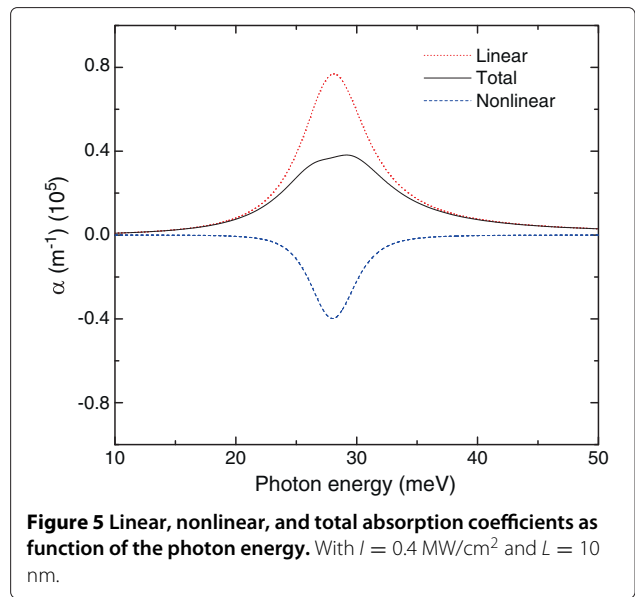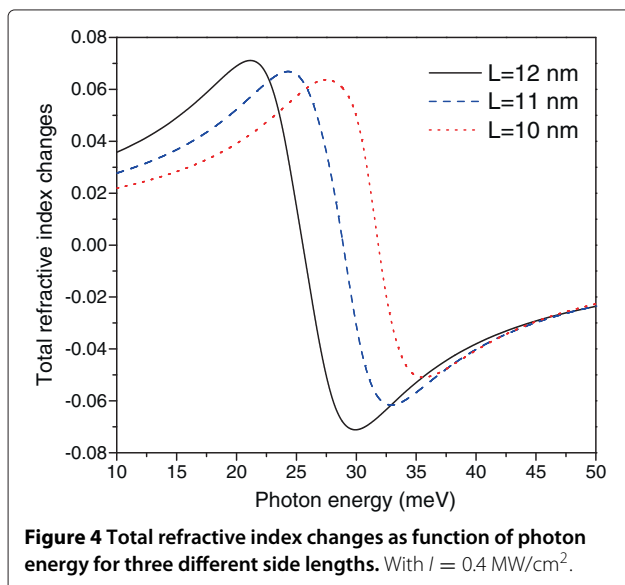
but the linear term is independent of the incident optical intensity.

In Figure 6, we have plotted the variations of the total absorption coefficient as a function of the photon energy for three different lengths as $L = 10, 11$, and 12 nm with $I = 0.4$ MW/cm^2. This figure clearly shows that the total absorption coefficient decreases as the quantum size L increases. One can see (Equations 25 and 26) that the absorption coefficients are strongly dependent on the dipole matrix elements M_{ij}. When the quantum size L increases, the wave function associated with the electron is more spread and less localized. Therefore, the dipole matrix elements and, thereby, the absorption coefficients

Figure 4 Total refractive index changes as function of photon energy for three different side lengths. With $I = 0.4$ MW/cm^2.

Figure 6 Total absorption coefficient as function of photon energy for three different side lengths. With $I = 0.4$ MW/cm^2.
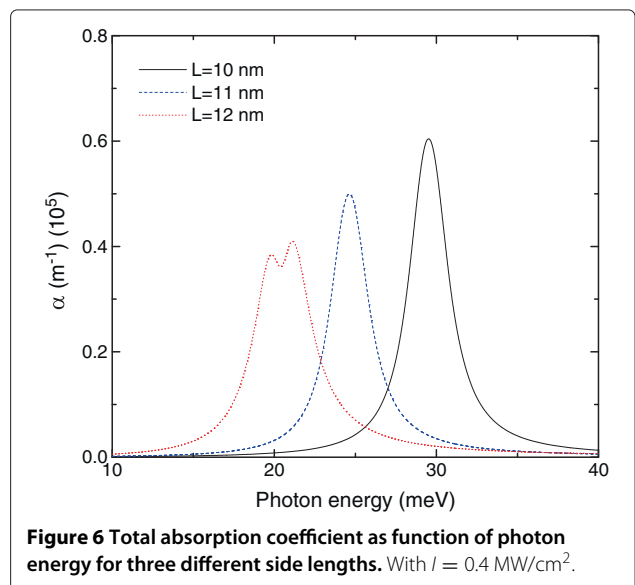
increase. From the figure, it is clear that the resonance peak position shifts towards lower energies with increasing quantum size L. The main reason for this behavior is the decrease of the quantum confinement with increasing L. Also, the energy difference between two electronic states reduces by increasing L. Therefore, the resonance peak position shifts towards lower energies.

Figure 7 displays the total changes in the absorption coefficient as a function of the photon energy for four different incident optical intensities as 0, 0.2, 0.4, and 0.6 MW/cm^2 with $L = 10$ nm. It is obvious from the figure that the total absorption coefficient reduces when the optical intensity increases. By increasing the optical intensity, the nonlinear absorption coefficient increases. Since the linear and nonlinear absorption coefficients are of opposite signs, the total absorption coefficient will be reduced. There is no shift in the resonance peak, but the saturation begins at $I = 0.6$ MW/cm^2.

Conclusion

In this work, we have solved the Schrödinger equation for an electron confined in a parallelogram quantum wire. We could obtain analytically the energy levels and wave functions. We have tried to study the linear, nonlinear, and total absorption coefficients and refractive index changes of this system. For this purpose, we have only considered the two-level system for electronic transitions. In summary, our results show that both the incident optical intensity and the structure parameter (L) have great effects on the total absorption coefficient and refractive index changes of a parallelogram quantum wire.
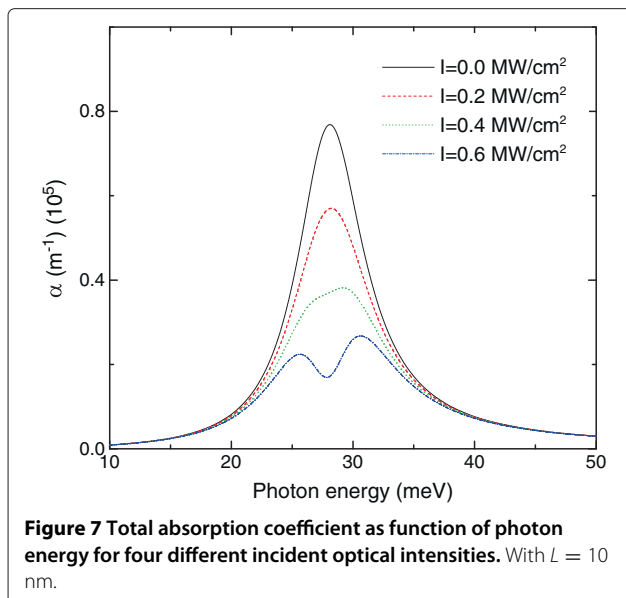

Figure 7 Total absorption coefficient as function of photon energy for four different incident optical intensities. With $L = 10$ nm.

Methods

Theory and model

The Hamiltonian of a charge carrier in a quantum wire is given by

$$H = -\frac{\hbar^2}{2m^*}\nabla^2 + V(x,y), \tag{1}$$

where m^* is the effective mass. Here, $V(x,y)$ is the confining potential (see Figure 1):

$$V(x,y) = \begin{cases} 0, & \text{Inside} \\ \infty, & \text{Outside} \end{cases}. \tag{2}$$

To obtain energy levels and wave functions, we should solve the Schrödinger equation in the cartesian coordinates.

$$-\frac{\hbar^2}{2m^*}\left[\frac{\partial^2}{\partial x^2} + \frac{\partial^2}{\partial y^2}\right]\psi(x,y) + V(x,y)\psi(x,y) = E\psi(x,y). \tag{3}$$

Let us consider a superposition of a finite number N of plane wave in two dimensions,

$$\psi(x,y) = \sum_{s=1}^{N} c_s \exp(i\alpha_s x + i\beta_s y), \tag{4}$$

where

$$\alpha_s^2 + \beta_s^2 = \lambda = \frac{2m^* E_s}{\hbar^2}, \qquad s = 1,2,...,N. \tag{5}$$

Amar et al. [32] applied a mathematical lemma to obtain the coefficients α_s, β_s and the energy levels λ. They considered a set of particular tilings of the plane, precisely those which are obtained by reflections of a single fundamental region (the reference tile). Using this procedure, we can generate a parallelogram of the plane starting from the reference tile and reflecting it successively in its sides. In the following paragraphs, we can explain this procedure

To generate a parallelogram, a copy of the reference tile along any side, say a_i, must necessarily exist due to the fact that the number of possible different geometrical postures which can be obtained by reflections of the reference tile is finite. If a_i and a_j are two adjacent sides of lengths $L(a_i)$ and $L(a_j)$, respectively, with reference to coordinate axes ζ and η along them, we must have the translation [32]

$$\zeta' = \zeta + p_i L(a_i), \qquad \eta' = \eta, \tag{6}$$

and

$$\zeta' = \zeta, \qquad \eta' = \eta + p_j L(a_j), \tag{7}$$

where p_i and p_j are integers. Considering the smallest p_i and p_j in Equations 6 and 7, a minimal parallelogram is naturally defined corresponding to each pair of adjacent sides. It is worth mentioning that Richard et al. [33] and Arnold et al. [34] used this procedure to generate convex plane polygons. In terms of cartesian coordinate axes x and y, if δ is the angle between a_i and a_j, the two independent translations can be written as

$$x' = x + p_i L(a_i), \qquad y' = y, \qquad (8)$$

and

$$x' = x + p_i L(a_i) \cos \delta, \qquad y' = y + p_j L(a_j) \sin \delta. \qquad (9)$$

With respect to Equations 4 to 9, the wave functions and energy levels can be written as

$$\psi(x, y) = \exp(\alpha x + \beta y), \qquad (10)$$

where

$$\alpha = 2n\pi / p_i L(a_i),$$
$$\beta = \frac{2m\pi p_i L(a_i) - 2n\pi p_j L(a_j) \cos \delta}{p_i p_j L(a_i) L(a_j) \sin \delta}. \qquad (11)$$

The corresponding eigenvalues are given by

$$\frac{2m^* E(n, m)}{\hbar^2} = \alpha^2(n, m) + \beta^2(n, m). \qquad (12)$$

Using geometrical considerations, the eigenvalues and eigenfunctions for a quantum wire with a parallelogram cross section can be written as [32-36]

$$\psi_{n,m}(x, y) = \sin[\frac{2\pi\sqrt{3}}{3L} nx] \sin[\frac{2\pi}{3L} my] - (-1)^{(m+2)/2}$$
$$\times \sin[\frac{2\pi\sqrt{3}}{3L} \frac{(m+n)}{2} x] \sin[\frac{2\pi}{3L} \frac{(3n-m)}{2} y]$$
$$+ (-1)^{(m+n)/2} \sin[\frac{2\pi\sqrt{3}}{3L} \frac{(n-m)}{2} x]$$
$$\sin[\frac{2\pi}{3L} \frac{(3n+m)}{2} x],$$

and

$$E(n, m) = (\frac{2\pi^2 \hbar^2}{9L^2 m^*})(3n^2 + m^2), \qquad (13)$$

where L is the side length. In the above equations, m and n are integers and have the following conditions:

$$n \neq 0, \qquad m \neq 0, \qquad m \neq \pm 3n, \qquad m \neq \pm n. \qquad (14)$$

Optical absorption coefficients and refractive index changes

In this section, we intend to use the density matrix formalism to calculate the refractive index changes and optical absorption coefficients of a quantum wire with a parallelogram cross section, related to an optical intersubband transition.

As we know, the system under study can be excited by an electromagnetic field of frequency ω, such as

$$E(t) = \tilde{E} e^{i\omega t} + \tilde{E}^* e^{-i\omega t}. \qquad (15)$$

The time evolution of the matrix elements of the one-electron density operator, ρ, can be written as [26, 27]

$$\frac{\partial \rho}{\partial t} = \frac{1}{i\hbar} [H_0 - qxE(t), \rho] - \Gamma(\rho - \rho^{(0)}), \qquad (16)$$

where H_0 is the Hamiltonian for this system without the electromagnetic field $E(t)$, and q is the electronic charge. The symbol $[,]$ is the quantum mechanical commutator; $\rho^{(0)}$ is the unperturbed density matrix operator; Γ is the phenomenological operator responsible for the damping due to the electron-phonon interaction, collisions among electrons, and etc. It is assumed that Γ is a diagonal matrix, and its elements are equal to the inverse of relaxation time T.

To solve Equation 17, Ahn et al. [37] applied the standard iterative method by expanding ρ as $\rho(t) = \sum_n \rho^{(n)}(t)$. Inserting this expansion into Equation 17, one can obtain density matrix elements as seen below:

$$\frac{\partial \rho_{ij}^{(n+1)}}{\partial t} = \frac{1}{i\hbar} [H_0, \rho^{(n+1)}]_{ij} - \Gamma_{ij} \rho_{ij}^{(n+1)} - \frac{1}{i\hbar} [qx, \rho^{(n)}]_{ij} E(t). \qquad (17)$$

After obtaining the density matrix ρ, we calculated the electronic polarization $P(t)$ and susceptibility $\chi(t)$ as

$$P(t) = \varepsilon_0 \chi(\omega) \tilde{E} e^{-i\omega t} + \varepsilon_0 \chi(-\omega) \tilde{E}^* e^{i\omega t} = \frac{1}{V} Tr(\rho M), \qquad (18)$$

where ρ and V are the one-electron density matrix and the volume of the system, ε_0 is the permittivity of free space, and the symbol Tr (trace) denotes the summation over the diagonal elements of the matrix.

Kuhn et al. [38] could obtain analytical forms of the linear $\chi^{(1)}$ and the third-order nonlinear $\chi^{(3)}$ susceptibility coefficients using Equations 18 and 19. To obtain more information about the calculation method of these coefficients, the reader can refer to [37, 38]. Kuhn et al. also

determined the refractive index changes using the real part of the susceptibility as

$$\frac{\Delta n(\omega)}{n_r} = Re \left[\frac{\chi(\omega)}{2n_r^2} \right], \qquad (19)$$

where n_r is the refractive index. The linear and the third-order nonlinear refractive index changes can be expressed as [38]

$$\frac{\Delta n^{(1)}(\omega)}{n_r} = \frac{\sigma_\upsilon \mid M_{21} \mid^2}{2n_r^2 \varepsilon_0} \left[\frac{E_{21} - \hbar\omega}{(E_{21} - \hbar\omega)^2 + (\hbar\Gamma_{12})^2} \right], \qquad (20)$$

and

$$\frac{\Delta n^{(3)}(\omega)}{n_r} = -\frac{\sigma_\upsilon \mid M_{21} \mid^2}{4n_r^3 \varepsilon_0} \frac{\mu c I}{\left[(E_{21} - \hbar\omega)^2 + (\hbar\Gamma_{12})^2 \right]^2}$$
$$\times \left[4(E_{21} - \hbar\omega) \mid M_{21} \mid^2 - \frac{(M_{22} - M_{11})^2}{(E_{21})^2 + (\hbar\Gamma_{12})^2} \right.$$
$$\times \left\{ (E_{21} - \hbar\omega) \left[E_{21}(E_{21} - \hbar\omega) - (\hbar\Gamma_{12})^2 \right] \right.$$
$$\left. \left. - (\hbar\Gamma_{12})^2 (2E_{21} - \hbar\omega) \right\} \right], \qquad (24)$$

where σ_υ is the carrier density, μ is the permeability, $E_{ij} = E_i - E_j$ is the energy difference, and $M_{ij} = | < \psi_i \mid qx \mid \psi_j > |$ is the electric dipole moment matrix element. In this present work, we have selected the polarization of the electric field in the x direction. Using Equations 21 and 22, one can write the total refractive index change as

$$\frac{\Delta n(\omega)}{n_r} = \frac{\Delta n^{(1)}(\omega)}{n_r} + \frac{\Delta n^{(3)}(\omega)}{n_r}. \qquad (21)$$

The absorption coefficient $\alpha(\omega)$ is also calculated from the imaginary part of the susceptibility $\chi(\omega)$ as

$$\alpha(\omega) = \omega \sqrt{\frac{\mu}{\varepsilon_R}} Im \left[\varepsilon_0 \chi(\omega) \right]. \qquad (22)$$

The linear and third-order nonlinear absorption coefficients can be written as [27, 39]

$$\alpha^{(1)}(\omega) = \omega \sqrt{\frac{\mu}{\varepsilon_R}} \left[\frac{\sigma_\upsilon \hbar\Gamma_{12} \mid M_{21} \mid^2}{(E_{21} - \hbar\omega)^2 + (\hbar\Gamma_{12})^2} \right], \qquad (23)$$

$$\alpha^{(3)}(\omega, I) = -\omega \sqrt{\frac{\mu}{\varepsilon_R}} \left(\frac{I}{2\varepsilon_0 n_r c} \right) \frac{\sigma_\upsilon \hbar\Gamma_{12} \mid M_{21} \mid^2}{[(E_{21} - \hbar\omega)^2 + (\hbar\Gamma_{12})^2]^2}$$
$$\times \left\{ 4 \mid M_{21} \mid^2 \right.$$
$$\left. - \frac{\mid M_{22} - M_{11} \mid^2 \left[3E_{21}^2 - 4E_{21}\hbar\omega + \hbar^2(\omega^2 - \Gamma_{12}^2) \right]}{E_{21}^2 + (\hbar\Gamma_{12})^2} \right\}, \qquad (24)$$

where I is the optical intensity of the incident wave, and it is given by

$$I = 2 \sqrt{\frac{\varepsilon_R}{\mu}} \mid E(\omega) \mid^2 = \frac{2n_r}{\mu c} \mid E(\omega) \mid^2, \qquad (25)$$

where c is the speed of light in free space. Using Equations 25 and 26, one can express the total absorption coefficient $\alpha(\omega, I)$ as [27, 37]

$$\alpha(\omega, I) = \alpha^{(1)}(\omega) + \alpha^{(3)}(\omega, I). \qquad (26)$$

References
1. Ferry, DK, Goodnick, SM: Transport in Nanostructures. Cambridge University Press, Cambridge (1997)
2. Imry, Y: Introduction to Mesoscopic Physics. Oxford University Press, Oxford (1997)
3. Bouhassoune, M, Charrour, R, Fliyou, M, Bria, D, Nougaoui, A: Polaronic and magnetic field effects on the binding energy of an exciton in a quantum well wire. J. Appl. Phys. **91**, 232–235 (2002)
4. Tanaka, M, Yamada, H, Maruyama, T, Akimoto, K: Well-width dependence of optical properties of rare-earth ion-doped $ZnS_{0.8}Se_{0.2}$/undoped ZnS multipole. Phys. Rev. B. **67**, 045305–045309 (2003)
5. Kasapoglu, E, Sari, H, Sokmen, I: Geometrical effects on shallow donor impurities in quantum wires. Physica E. **19**, 332–335 (2003)
6. Feng, DH, Xu, ZZ, Jia, TQ, Li, XX, Gong, SQ: Quantum size effects on exciton states in indirect-gap quantum dot. Phys. Rev. B. **68**, 035334–035340 (2003)
7. Khordad, R, Gharaati, A, Haghparast, M: Polarizability of a hydrogenic donor impurity in a ridge quantum wire. Current Appl. Phys. **10**, 199–202 (2010)
8. Angelova, T, Cros, A, Cantarero, A, Fuster, D, González, Y, González, L: Raman study of self-assembled InAs/InP quantum wire stacks with varying spacer thickness. J. Appl. Phys. **104**, 033523–033528 (2008)
9. He, J, Krenner, HJ, Pryor, C, Zhang, JP, Wu, Y, Allen, DG, Morris, CM, Sherwin, MS, Petroff, PM: Growth, structural, and optical properties of self-assembled (In,Ga)As quantum posts on GaAs. Nano Lett. **7**, 802–806 (2007)
10. Fabian, J, Matos-Abiague, A, Ertler, C, Stano, P, Zutic, I: Semiconductor spintronics. Acta Phys. Slovaca. **57**, 565–907 (2007)
11. Zutic, I, Fabian, J, Das, Sarma, S: Spintronics: fundamentals and applications. Rev. Mod. Phys. **76**, 323–410 (2004)
12. Fabian, J, Zutic, I, Das, Sarma, S: Magnetic bipolar transistor. Appl. Phys. Lett. **84**, 85–87 (2004)
13. Karabulut, I, Atav, U, Safak, H, Tomak, M: Linear and nonlinear intersubband optical absorption in an asymmetric rectangular quantum well. Eur. Phys. J. B. **55**, 283–288 (2007)
14. Rezaei, G, Vaseghi, B, Khordad, R, Azadi, Kenary, H: Optical rectification coefficient of a two-dimensional quantum pseudodot system. Physica E. **43**, 1853–1856 (2011)
15. Levine, BF, Malik, RJ, Walker, J, Choi, KK, Bethea, CG, Kleinman, DA, Vandenberg, JM: Strong 8.2 m infrared intersubband absorption in doped GaAs/AlAs quantum well waveguides. Appl. Phys. Lett. **50**, 273–275 (1987)
16. Harwitt, A, Harris, JS: Observation of Stark shifts in quantum well intersubband transitions. Appl Phys. Lett. **50**, 685–687 (1987)
17. Ahn, D, Chuang, SL: Nonlinear intersubband optical absorption in a semiconductor quantum well. J. Appl. Phys. **62**, 3052–3055 (1987)
18. Rappen, T, Schröder, J, Leisse, A, Wegener, M, Schäfer, W, Sauer, NJ, Chang, TY: Nonlinear absorption of two-dimensional magnetoexcitons in

$In_xGa_{1-x}As/In_yAl_{1-y}As$ quantum wells. Phys. Rev. B. **44**, 13093–13096 (1991)

19. Bockelmann, U, Bastard, G: Interband absorption in quantum wires. II. Nonzero-magnetic-field case. Phys. Rev. B. **45**, 1700–1704 (1992)

20. Bockelmann, U, Bastard, G: Interband absorption in quantum wires. I. Zero-magnetic-field case. Phys. Rev. B. **45**, 1688–1699 (1992)

21. Yuh, PF, Wang, KL: Intersubband optical absorption in coupled quantum wells under an applied electric field. Phys. Rev. B. **38**, 8377–8382 (1988)

22. Cui, DF, Chen, ZH, Pan, SH, Lu, HB, Yang, GZ: Absorption saturation of intersubband optical transitions in $GaAs/Al_xGa_{1-x}As$ multiple quantum wells. Phys. Rev. B. **47**, 6755–6757 (1993)

23. Khordad, R, Tafaroji, S, Katebi, R, Ghanbari, A: Optical and electronic properties of anisotropic parabolic quantum disks in the presence of tilted magnetic fields. Physica B. **407**, 533–538 (2012)

24. Khordad, R: Pressure effect on optical properties of modified Gaussian quantum dots. Physica B. **407**, 1128–1133 (2012)

25. Xie, W, Liang, S: Optical properties of a donor impurity in a two-dimensional quantum pseudodot. Physica B. **406**, 4657–4660 (2011)

26. Wang, GH, Guo, Q, Guo, KX: Refractive index changes induced by the incident intensity in semiparabolic quantum well. Chin. J. Phys. **41**, 296–306 (2003)

27. Ünlü, S, Karabulut, İ, Safak, H: Linear and nonlinear intersubband optical absorption coefficients and refractive index changes in a quantum box with finite confining potential. Physica E. **33**, 319–324 (2006)

28. Karabulut, I, Baskoutas, S: Linear and nonlinear optical absorption coefficients and refractive index changes in spherical quantum dots: Effects of impurities, electric field, size, and optical density. J. Appl. Phys. **103**, 073512–073516 (2008)

29. Khordad, R: Effect of position-dependent effective mass on linear and nonlinear optical properties in a quantum dot. Indian J. Phys. **86**, 513–519 (2012)

30. Karabulut, I, Safak, H, Tomak, M: Nonlinear optical rectification in asymmetrical semiparabolic quantum well. Solid State Commun. **135**, 735–738 (2005)

31. Khordad, R, Bijanzadeh, A: Optical absorption spectra related to donor impurities in $GaAs/Ga_{1-x}Al_xAs$ ridge quantum wire. Mod. Phys. Lett. B. **23**, 3677–3685 (2009)

32. Amar, V, Pauri, M, Scotti, A: Schrödinger equation for convex plane polygons: a tiling for the derivation of eigenvalues and eigenfunctions. J. Math. Phys. **32**, 2442–2449 (1991)

33. Richens, PJ, Berry, MV: Pseudointegrable systems in classical and quantum mechanics. Physica D. **2**, 495–512 (1981)

34. Arnold, VI, Avez, A: Ergodic Problems of Classical Mechanics. Benjamin, New York (1968)

35. Li, WK, Blinder, SM: Solution of the Schrödinger equation for a particle in an equilateral triangle. J. Math. Phys. **26**, 2784–2786 (1985)

36. Gorley, PN, Vorobiev, YV, Hernández, JG, Horley, PP: Analytical solution of the Schrödinger equation for an electron confined in a triangle-shaped quantum well. Microelec. Engin. **66**, 39–44 (2003)

37. Ahn, D, Chuang, S. L: Calculation of linear and nonlinear intersubband optical absorptions in a quantum well model with an applied electric field. IEEE J. Quant. Elect. **23**, 2196–2199 (1987)

38. Kuhn, KJ, Lyengar, GU, Yee, S: Free carrier induced changes in the absorption and refraction index for intersubband optical transitions in $Al_xGa_{1-x}As/GaAs/Al_xGa_{1-x}As$ quantum wells. J. Appl. Phys. **70**, 5010–5017 (1991)

39. Aspnes, DE: GaAs lower conduction-band minima: ordering and properties. Phys. Rev. B. **14**, 5331–5343 (1976)